Noise Immunity Analysis of the Forward Hadron Calorimeter Front-End Electronics

C. Rivetta*, F. Arteche**, F. Szoncso **

*FERMILAB, P.O Box 500 MS222, Batavia Il 60510 USA, **CERN,1211 Geneve 23 Switzerland;
(Principal contacts: rivetta@fnal.gov, fernando.arteche@cern.ch)

Abstract

The Very Forward Hadron Calorimeter (HF) in CMS is composed by about 3000 photo-multipliers (PMT) arranged in boxes housing 24 PMTs each one. Read-out amplifiers are arranged in 6 channel daughter cards located about 4 meters from the PMTs. Shielded cables are used to connect the PMT anode signal to the amplifiers.

This paper addresses the study of the immunity to common mode spurious signal and external fields of the electronic system described above. It allows predicting grounding and shielding problems and estimating the effect of interference noise at early stages of the design.

I. INTRODUCTION

The front-end electronics (FEE) of the HF detector is composed by photo-multipliers (PMT) located about 4 mts. from the sensitive amplifiers. PMTs are biased using a resistive divider and its gain can be adjusted between $4x10^5$ and $5x10^6$. High Voltage power supplies are located into the counting room about 120 mts. from the metallic boxes housing the PMTs. The anode current is amplified and digitised by a special gated charge amplifier. This ASIC chip, denominated Charge Integrator Encoder (QIE) is a differential current mode amplifier with an input impedance of either 93 Ω or 50 Ω for the frequency span of 40MHz and the full input current range. The sensitivity of this amplifier is 2.7fC/LSB and it integrates the signal during a period of 25nsec. The dynamic range of each input current is asymmetric, positive currents in both inputs can be processed to obtain an output charge of 27pC, while negative currents can reach only a few fC. Due to the asymmetric dynamic range, two cables with its own current return have to be used to complete the differential topology. The complete circuit for one channel is depicted in figure 1.

Amplifiers are grouped in 6 channel cards and more than 10 boards are housed in small crates. All the amplifier cards are locally grounded at the detector ground. The box holding the PMTs is also locally grounded at the detector structure but about 4 mts from the ground connection of amplifiers. As it is depicted in figure 1, each return point of the PMTs is isolated from the ground connection through the resistor R_{GND}.

The signal connection between each PMT and the respective amplifier has to fulfil not only the wide-band requirement for signal fidelity but also has to be able to provide enough common mode rejection to avoid amplification of spurious signal due to the remote connection between grounds. The purpose of this paper is to present the assessment of electromagnetic compatibility in the early state of the electronic design. As illustration, we choose the connection between PMTs and QIE for the CMS very forward calorimeter. These wide band amplifiers are very sensitive and the tolerated noise in the detector is just above the intrinsic thermal noise of the QIEs. Any interference noise must be kept very low in order to fulfil the dynamic range and performance requirements.

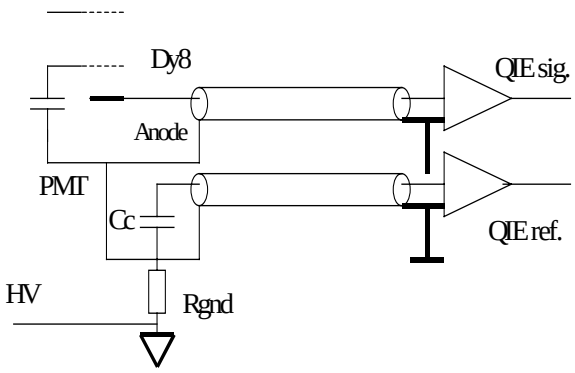

Figure 1 . Layout PMTs - QIE

The quality of the differential structure depends on the balance of both signal paths and the magnitude of the resistor R_{GND}. The influence of these parameters has been studied by simulation using a model of the cables based on the multi-transmission line theory. The common mode rejection of the topology is analysed and its sensitivity to parameter variations and un-matching is addressed. The effects of external magnetic and electric field could cause interference in the system, which result in poor performance of the FEE. These effects have been included in the simulations to establish the immunity level of the connection against external electromagnetic fields. These quantitative studies are important to design a system with high immunity and address the susceptibility to interference noise during the design stage.

II. CONSIDERATIONS ABOUT NOISE

The noise level defines the minimum signal that the front-end electronics can process. The noise at the front-end electronics is due to the contribution of different sources and perturbations as: thermal noise of transistors and resistors, noise picked-up by connections between the sensor devices and the FEE, spurious signals, etc. Taking as a common point the analogue output stage of the QIE to analyse the total noise, it can be written as:

$$n_a(t) = n_{th}(t) + n_{cm}(t) + n_{emi}(t) + ... \quad (1)$$

where *nth(t)* is the thermal noise contribution, $n_{cm}(t)$ is the noise due to common mode signals, and $n_{emi}(t)$ represent the contribution due to electromagnetic interference (EMI). These three terms are the more important in this analysis.

The thermal noise is characterized by the power spectral density

$$N_{th}^2(\omega) = 2.\left[\left| Tv(\omega) \right|^2 .e_n^2(\omega) + \left| Ti(\omega) \right|^2 .i_n^2(\omega) \right].\left| Tamp(\omega) \right|^2; \quad (2)$$

where e_n^2 (ω) and i_n^2(ω) are the spectral density of the equivalent series and parallel thermal noise generators of the QIE.

The additional noise due to common mode signals and EMI can be represented mathematically as:

$$\begin{aligned} Ncm(\omega) &= Tcm(\omega).Tamp(\omega).Vcm(\omega) \\ Nemi(\omega) &= \left[TemiH(\omega).H(\omega) + TemiE(\omega).E(\omega) \right] Tamp(\omega) \end{aligned} \quad (3)$$

where *Tcm(ω):* is common mode transference, *Tamp(ω):* QIE transference, *TemiH (ω) , TemiE(ω):* output voltage to magnetic field and electric field transference, respectively.

The criteria generally used to define the total noise contribution in a design is to define the total noise mainly due to the thermal noise, making any external noise perturbation much lower that the thermal noise. It is

$$\left\langle na^2 \right\rangle \cong \left\langle nth^2 \right\rangle; \qquad \left\langle (ncn + nemi + ...)^2 \right\rangle \to 0 \quad (4)$$

In order to use this criterion for the design it is necessary to know and minimize $\left\langle nth^2 \right\rangle$ and to define the factors $Tcm(\omega)$, $TemiH(\omega)$ and $TemiE(\omega)$ to reduce their contribution in the total noise.

III. THERMAL NOISE

The QIE is a differential amplifier where each input current is amplified and integrated by 25nsec. Defining *i+* and *i-*, the input currents of the QIE, *C* the integration capacitance and *g(t)* the impulsive response of the input stage, the signal at the output of the analogue stage is given as:

$$v_a(t) = \frac{1}{C} \int_0^{\tau} g(t) * (i_+(t) - i_-(t)).dt \quad (5)$$

where τ is the integration period and '*' denotes the convolution operation. Applying Laplace transform, eqn. 5 can be written as:

$$V_a(s) = \frac{1 - e^{-s.\tau}}{s} . \frac{G(s).\left[I_+(s) - I_-(s) \right]}{C} = T_{amp}(s).\left[I_+(s) - I_-(s) \right]$$

where G(s) is the Laplace transform of g(t). The QIE transference, *Tamp*(ω), can be evaluated in frequency domain replacing the complex frequency *s* by $s = j.w = j.2.\pi.f$,with $j = \sqrt{-1}$.

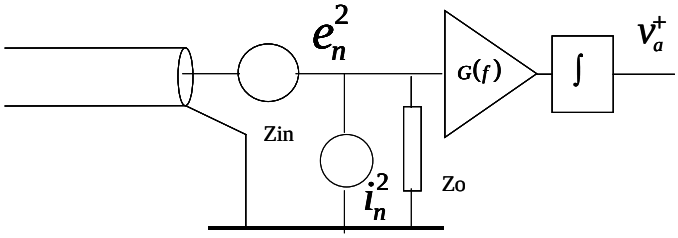

Figure 2. Equivalent circuit to calculate the thermal noise

To calculate the thermal noise, each branch of the QIE differential circuit can be modelled as indicated in figure 2. The coaxial cable is considered in open-circuit at the sending-end and the impedance presented to the input is:

$$Z_{in}(\omega) = -j.Z_0.ctg(\beta.L) \quad (6)$$

where $\beta = \omega / vel.$ is the propagation constant. The input impedance of the amplifier Zo is matched to the coaxial cable characteristic impedance. The amplifier noise is characterized by two independent sources that represent the equivalent series and parallel thermal noise. The current at any QIE input, in frequency domain, is:

$$i_{in} = \frac{e_n(\omega)}{(Z_{in} + Z_o)} + \frac{i_n(\omega).Z_{in}}{(Z_{in} + Z_0)} = Tv(\omega).e_n(\omega) + Ti(\omega).i_n(\omega) \quad (7)$$

giving a power spectral density at the output of the analogue stage as expressed by eqn 2. The normalized output power noise can be defined as:

$$\left\langle nth^2 \right\rangle = \int_0^{\infty} N_{th}^2(\omega).df \quad (8)$$

and the solutions of this equation for *G(ω)=G=cte*. Are:

$$\left\langle nth^2 \right\rangle = \frac{G^2}{C^2} . \left(\frac{e_n^2}{|Z_o|^2} + i_n^2 \right) . \frac{\tau}{4} \quad \text{if } \beta.\mathrm{L} \geq \frac{\omega.\tau}{2}$$

and

$$\left\langle nth^2 \right\rangle = \frac{G^2}{C^2} . \left\{ \left(\frac{e_n^2}{|Z_o|^2} - i_n^2 \right) . \frac{L}{2.vel} + i_n^2 . \frac{\tau}{2} \right\} \quad \text{if } \beta.\mathrm{L} < \frac{\omega.\tau}{2}$$

From these equations, it is important to note if $\beta.L \geq \omega.\tau/2$, the length of the cable has not influence on the output power noise. In addition, the output power noise decreases if the characteristic impedance of the cable increases.

IV. MULTI-TRANSMISSION LINE MODEL

The present studies are based on the multi-conductor transmission line (MTL) theory. This model assumes transverse electromagnetic (TEM) wave as propagation mode. It allows representing the cable in per-unit parameters that are relatively easy to measure or calculate given the geometry of the cable. A detailed analysis of MTL is presented in [1] [2] [3].

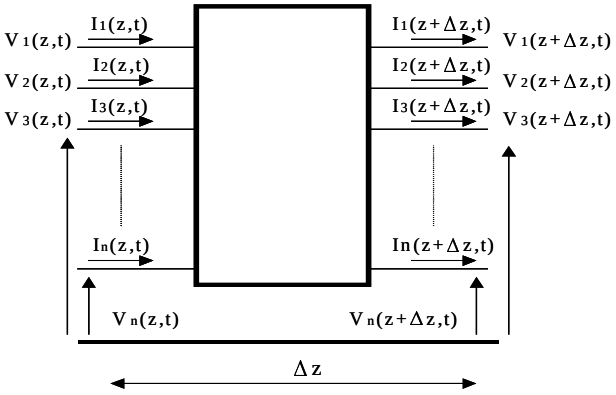

Figure. 3. Scheme of a differential sector of a MTL

Assuming a MTL sector with infinitesimal length, *Δz,* as it is depicted in figure 3, the system can be modelled by the partial differential equation.

$$\frac{\partial}{\partial z}V(z,t) = -R\,I(z,t) - L\frac{\partial}{\partial t}I(z,t)$$
$$\frac{\partial}{\partial z}I(z,t) = -GV(z,t) - C\frac{\partial}{\partial t}V(z,t) \qquad (9)$$

where *I(z,t)* and *V(z,t)* are vectors representing the current and the voltage respect to the reference conductor, respectively*; L, C, R, G,* are the per-unit-length inductance, capacitance, resistance, and conductance NxN matrices, respectively, that contain the cross-sectional dimensions and properties of the line, *z* is the position along the transmission line and *t* denotes the time variable.

The procedure to solve the eqn. 9 is to obtain the general solution of the MTL equations in time-domain or frequency-domain and then incorporate the terminal network constraints in that general solution to determine the line voltages and currents at the both ends of the line. All the analysis in this paper is conducted in frequency-domain.

V. SURFACE TRANSFER IMPEDANCE

The model presented above does not include the coupling effect in the central conductors of currents flowing through the shield. The equivalent circuit of figure 4 represents this coupling mechanism based on MTL theory for a sector of line of infinitesimal length [4]. The circuit consists of the inner system representing the central conductor of the coaxial cable and the braided shield as reference conductor. The outer system (shield - trays) is considered as a transmission line, where the metallic tray is the reference of the outer system and the shield is the conductor

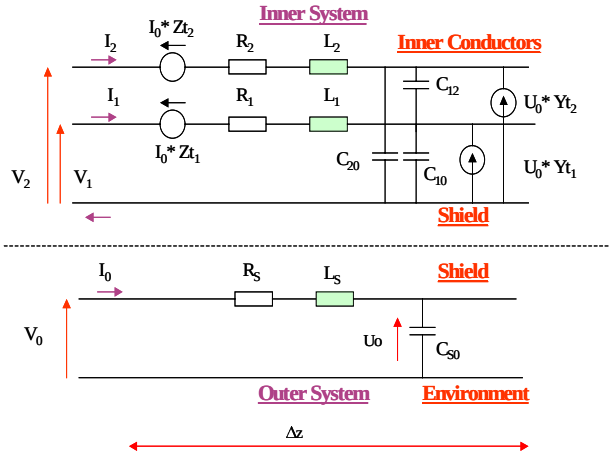

Figure 4. Inner conductor - Shield -Environment equivalent circuit.

The voltage and current sources at each inner conductor represent the interaction between both inner and outer systems. *Zt* and *Yt* represent the surface transfer impedance and the surface transfer admittance. The transfer impedance (*Zt*), is defined as the ratio between the voltage of the inner conductor i respect to the shield and the current flowing through the shield, per unit length. The transfer admittance is defined as the ratio between the current flowing through the inner conductor and the voltage between the shield and the environment, per unit length. The last magnitude is generally very small and it has not been considered in the present study. Both, the surface transfer impedance and admittance are characteristic parameters of the shield of the cable.

The transfer impedance depends on three components as defined by the equation [5][6][7][8].

$$Zt = Zd(\omega) + j.\omega.(Mh \pm Mb) \qquad (10)$$

where: $Zd(\omega)$: The *diffusion coupling component* is due to skin effect in the shield. It is predominant at low frequencies.

Mh : The *aperture-coupling component* is defined as the coupling through the holes of the shield. It plays an important role in the value of the transfer impedance at high frequencies.

Mb : The *braid inductance component* is defined as the coupling between the external and the internal layers of the shield.

To include the effect of the surface transfer impedance and admittance in the inner conductors, the mathematical model defined by eqn 9 is augmented by the generators *Zt.Io(z,t)* and *Yt.Uo(z,t)*.

$$\frac{\partial}{\partial z}V(z,t) = -R\,I(z,t) - L\frac{\partial}{\partial t}I(z,t) + Zt.Io(z,t)$$
$$\frac{\partial}{\partial z}I(z,t) = -GV(z,t) - C\frac{\partial}{\partial t}V(z,t) + Yt.Uo(z,t) \qquad (11)$$

The solution of the complete system of equations starts with the solution of the outer system, calculating the distributed voltage *Uo(z,t)* and the distributed current *Io(z,t)* at every location *z* of the outer system. These voltages and currents are used to calculate the magnitude of the additional generators defined in eqn. 11. Based on that, the solution of eqn. 11 follows a similar procedure than the solution of eqn. 9.

VI. COMMON MODE REJECTION - EXAMPLES

For the present study the coaxial cable RG-58U has been chosen to connect the PMTs and the QIE. It is the most common coaxial cable and there is plenty of information and tests about this cable that allowed a simple validation of the model used in this study. For future studies, the final cable will be used and in that case, it will be necessary to extract the appropriated model and parameters.

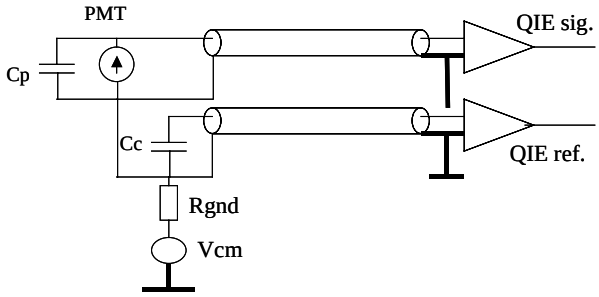

Figure. 5 Equivalent circuit to analyse the common mode rejection

The common mode rejection of the differential topology has been studied considering the circuit depicted in figure 5. The effects of unbalances are studied considering a mismatch between the parasitic capacitance of the PMT anode, socket and board, *Cp* and the compensation capacitance *Cc*. In addition, the relative position of the coaxial cables respect to the reference tray is analysed assuming the coaxial cables are placed at different heights respect to the reference. In all cases, the resistor R_{GND} is changed to quantify its effect in the common mode rejection.

The common mode rejection T_{CM} of the circuit is defined as:

$$T_{cm} = 20 \cdot Log_{10}\left(\frac{Va}{Vcm}\right)$$

Figure 6 depicts the common mode transfer function, T_{cm}, for a frequency range between 1kHz and 100 MHz, for different values of R_{GND} (100Ω, 1kΩ, 10kΩ), with the parasitic capacitance *Cp* different of *Cc*. The R_{GND} has a big influence in the common mode rejection of the system at low frequencies, however there is no significant difference between the different configurations for frequencies higher than 20 MHz.

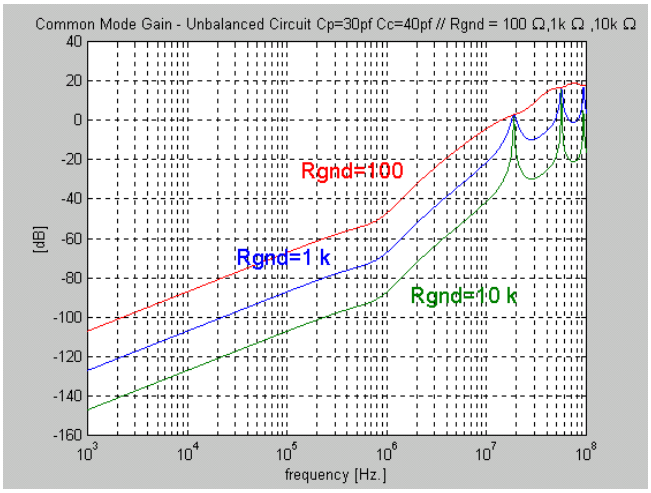

Figure 6. Common mode rejection - Unbalanced Circuit (Cp-Cc) with different R_{GND} values

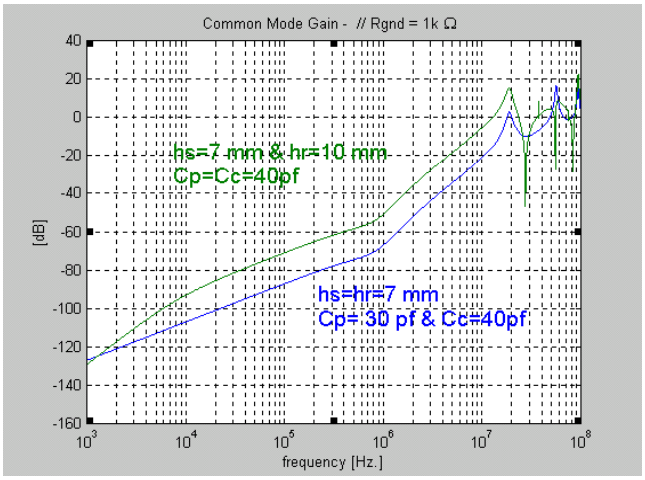

Figure 7. Common mode rejection for different position of cables

Unbalances due to the position of both coaxial cables respect to the metallic tray, reduce the capacity of the system to reject common mode signals. This effect is due to the currents flowing through the coaxial cable shields are not equal coupling different voltages in the central conductors. Figure 7 depicts T_{cm} for two different configurations. One of them is a system with the capacitances perfectly balanced but with the coaxial cables placed at different heights (7 mm & 10 mm). The other has unbalanced capacitances but both coaxial cables are placed at the same level. In both cases, R_{GND} was fixed at 1kΩ.

In both plots depicted above, the QIE is assumed as a perfect amplifier with infinite common mode rejection and

bandwidth. The effect of finite common mode rejection of the QIE will increase T_{cm} at low frequencies, while the effect of finite bandwidth dominated by the 25 nsec integration time is introduced in figure 8. In this figure, T_{CM} depicts the common mode rejection assuming an ideal QIE, while T_{CM}·T_{AMP} includes the frequency response of the QIE.

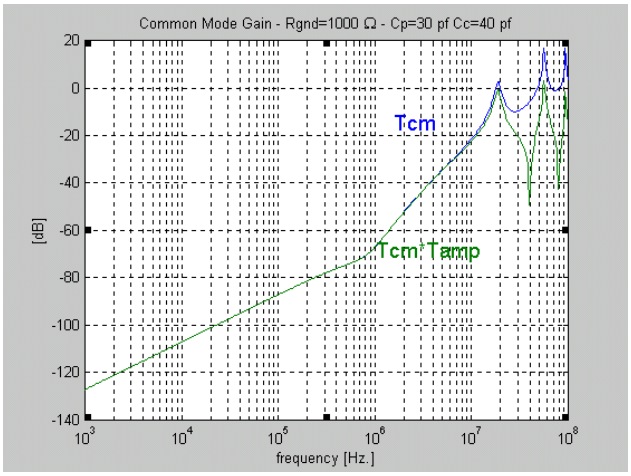

Figure 8. Common mode rejection - Ideal & Real QIE

VII. EXTERNAL ELECTROMAGNETIC FIELD

The effect of coupling external electromagnetic fields into a multi-conductor transmission line is well described in [3] [9]. The coupling effect into two-conductor transmission lines was first introduced by Clayton in [2] and later extended to multi-conductor lines by [10] C.W Harrison and to shielded cables by Vance [5]. A short description of the most important aspects is presented here.

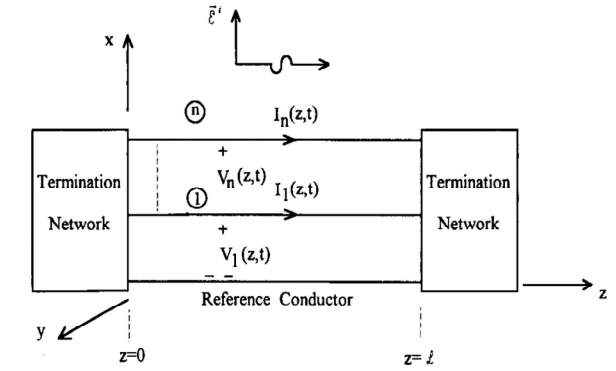

Figure 9. Reference model to evaluate the EMI in MTL

The effects of the incident field are configured as distributed sources along the line. These effects appear as forcing functions on the right-hand side of the MTL equations. To considerer the geometry of the system and the incidence of the electromagnetic wave, a reference system as depicted in figure 9 is used.

The MTL equations including the external electromagnetic fields effects are:

$$\frac{\partial}{\partial z}V(z,t)+L\frac{\partial}{\partial t}I(z,t)+RI(z,t)=V_F(z,t)$$
$$\frac{\partial}{\partial z}I(z,t)+C\frac{\partial}{\partial t}V(z,t)+GV(z,t)=I_F(z,t) \quad (12)$$

where the N x 1 vectors on the right hand sides, $V_F(z,t)$ and $I_F(z,t)$, model the effects of the incident fields and are determined by the components of incident electric and magnetic fields that lie in the transverse plane (the x, y plane normal to the z-axis of the line) and the geometry of the cables respect to the reference. The procedure to solve eqn. 12 is very similar to the one described to solve eqn. 11. After defining the distributed voltages $V_F(z,t)$ and currents $I_F(z,t)$, the magnitude the current flowing through the shield is calculated. With this current and the magnitude of the transfer impedance of cables, the voltages at the sending-end and the receiving-end of the lines can be calculated similarly to the analysis of point V.

VIII. EXTERNAL ELECTROMAGNETIC FIELD - EXAMPLES

In this example, the wave is propagating in the positive direction of *z* with the electric field polarised in the positive direction of *x* and the magnetic field perpendicular to the plane created by the cable and the metallic tray, which has been chosen as a reference plane. The case under study is referred as electromagnetic plane wave with an end-fire excitation.

The distributed voltages and currents in frequency domain $V_F(z)$ and $I_Z(z)$ are calculated assuming a plane wave and a constant electric field Eo for all frequencies. For the end-fire excitation field it is:

$$V_F(z)=2h\hat{E}_0\left[\frac{Sin(\beta_x h)}{\beta_x h}\right]e^{-j\beta_z Z}(j\beta_z e_x-j\beta_x e_z)$$
$$I_F(z)=-j2C.h.\ \hat{E}_0\left[\frac{Sin(\beta_x h)}{\beta_x h}\right]e^{-j\beta_z Z}(e_x) \quad (13)$$

where *ex*, *ey*, *ez* are the normalized projections of the electric field vector on the rectangular coordinate system., $\beta=\omega\sqrt{\mu\varepsilon}$, propagation constant and *h* cables height respect to the reference. In this example, $e_x=1 \quad e_y=e_z=0$. The magnitude of the electric field applied is 100μV/m, which corresponds to the limit emission level suggested by the EN 55022 B standard.

Figure 10 depicts the effect of the incident electromagnetic wave in the system when the capacitances *Cp* and *Cc* are not equal. The resistor R_{GND} has low influence rejecting this perturbation.

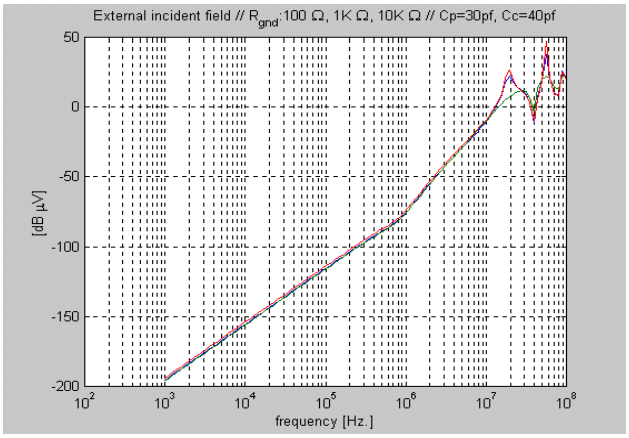

Figure 10. Effect of EMI for unbalanced Circuit (Cp-Cc) with different R_{GND} values

The influence of unbalances generated by the different position of the cables on the cable tray degrades the performance of the differential amplifier more than the capacitance unbalance. The effect of the cables heights is compared in figure 11 with the effect of different capacitances for a resistor R_{GND}=1KΩ.

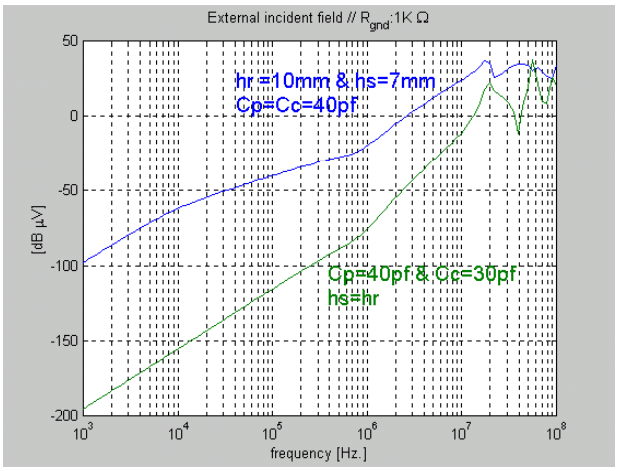

Figure 11. Effect of EMI for different cables heights

IX. CONCLUSIONS

This paper has presented a preliminary noise immunity analysis of the differential amplifier to be used by the FEE of CMS very forward calorimeter. The influence of common mode spurious signal and EMI has been conducted by simulation using a line model based on the MTL theory. Results have shown the limitations of the topology to common mode rejection and EMI if it is implemented with separated coaxial cables. It was shown that the position of the cable respect to the reference plane has strong influence in the rejection of the differential amplifier. The rejection can be improved selecting cables with double screening that balance the outer circuit impedance for both cables conforming the differential pair.

Based on these simulation tools a quantitative study of noise sensitivity of the final topology will be conducted. In addition, improvements will be included to the simulation program to allow time-domain solutions, in order to have a general tool to analyse quantitatively different problem involving connection between sensitive systems via cables.

X. ACKNOWLEDGEMENTS

One of the authors (C.R.) wants to thank to Fermilab PPD-EED for the support to complete this work. This work was performed under contract # DEACO2-76CH03000 with the Department of Energy – USA.

XI. REFERENCES

[1]- Antonije R. Djordjevic, Tapan K. Sarkar and Roger F. Harrington" *Time domain Response of Multi-conductor Transmission Lines*" , Proc. IEEE 1987, Vol 75 pp. 743 - 763

[2]- C.R. Paul, *Introduction to Electromagnetic Compatibility* NY: Wiley-Interscience, 1992, ISBN-0-471-54927-4

[3]- C.R. Paul." *Analysis of multi-conductor transmission lines* ", 1994

[4]- Lorenz-Jung, Jan Luiken ter Haseborg " *Evaluation of measured complex transfer admittance for the characterisation of shield in-homogeneities of Multi-conductor Cables* ", IEEE Trans, on Electromagnetic Compatibility vol. 41 No 4 - Nov.1999

[5]- Edward F. Vance " *Coupling to shielded cables* ", 1987, ISBN 0-89874-949-2.

[6]- Goedbloed, Jasper J. "*Electromagnetic Compatibility*", 1990, ISBN-0-13-249293-8.

[7]- Tyni, M." *The transfer impedance of coaxial with braided outer conductor*", Pr. Nauk, Inst Telekomun Akust. Politech Wroclaw Ser. Konfi pp 410-419, 1975.

[8]- S.Sali, "*An improve Model for the Transfer Impedance Calculations of Braided Coaxial Cables"* IEEE Transactions on Electromagnetic Compatibility vol. 33 No 2 - May.1991.

[9]- Ashok K. Agrawal , Harold J. Price, Shyam H. Gurbaxami " *Transient Response of Multi-conductor Transmission Lines Excited by Non-uniform Electromagnetic Fields* ", IEEE Transactions on Electromagnetic Compatibility vol. 22 No 2 - May.1980

[10]- C.W. Harrison, "*Generalised theory of impedance loaded mult-conductor transmission lines in an incident field "* IEEE Transactions on Electromagnetic Compatibility vol. 14, pp 56-63 - May.1972